UNNS Substrate Research Program | Working Manuscript

Color Confinement as Admissibility-by-Closure: A UNNS Boundary-Route Interpretation

Instruments: STRUC-I v1.0.4 · STRUC-PERC-I v2.5.0

Diagnostic corpus: 57 static energy-level rows · 1,090 flux pointwise rows (41 profiles) · 9 chamber-ready ladders

Primary sources: Bulava (2019, 2024) · Baker (2024) · Cardoso (2013, queued)

Status: Conceptual manuscript with bounded diagnostic support · Date: July 2026

Abstract

Color confinement — the absence of isolated colored states in the observable hadron spectrum — is treated here not as a phenomenon to be derived, but as a physical benchmark case for the UNNS Substrate principle of *admissibility-by-closure* (UNNS = Unbounded Nested Number Sequences). The central claim is structural, not dynamical: an internally real colored coordinate is not an admissible external output; attempted route extension toward isolation produces localized route tension; that tension resolves at a repair-threshold window into an admissible color-neutral composite route. Symbolically,

$$\begin{gathered}\text{internal colored coordinate} \to \text{attempted route extension}\\ \to \text{localized route tension} \to \text{repair-threshold window}\\ \to \text{admissible color-neutral composite route.}\end{gathered}$$

This manuscript does not derive QCD confinement, does not replace lattice QCD or gauge theory, and does not treat any UNNS quantity as a QCD potential. It uses a single derived diagnostic coordinate, $\Pi_{\text{boundary}}(r)$, built from source-indexed static-source energy levels and flux-tube profiles, to test whether repair-window information can be coordinatized into a stable, fully connected UNNS boundary-pressure ladder. Under the STRUC-I admissibility chamber and the STRUC-PERC-I connectivity chamber, the derived coordinate is simultaneously chamber-stable ($A_\kappa = 1.000$) and fully connected (giantRatio = 1.000). No raw local descriptor in the corpus achieves the same exact joint profile: perfect STRUC-I stability with min $A_\kappa = 1.000$ and STRUC-PERC-I FULL_PERCOLATION. The static-source spectrum used is model-reconstructed from published Hamiltonian parameters, not raw GEVP lattice output, and the empirical section is presented accordingly as a bounded, source-indexed diagnostic exercise rather than a new lattice-QCD analysis.

Keywords: admissibility-by-closure; boundary-pressure coordinate; route repair; color confinement; string breaking; UNNS Substrate; STRUC-I; STRUC-PERC-I.

1 Introduction

1.1 Scope of the claim

This paper makes a narrow and explicit claim, stated here before any physics or diagnostics are introduced, so that it cannot be read more broadly than intended.

- This paper does not derive QCD confinement.

- It does not replace lattice QCD or the gauge-theoretic account of color confinement.
- It treats color confinement as a physical benchmark against which the UNNS notion of *admissibility-by-closure* can be tested and illustrated.

This restriction is not a rhetorical hedge; it reflects the actual status of the supporting material. The empirical package underlying §7–§9 is documented, in its own internal provenance records, as a *data seed* — a source-indexed collection of published static-source energy levels and flux-tube profiles reorganized for diagnostic use — and not as a raw lattice-data repository. The static-source energy levels used are model-reconstructed from reported Hamiltonian parameters, not raw Generalized Eigenvalue Problem (GEVP) lattice points. Every claim in this manuscript is written to remain true under that constraint.

1.2 The central thesis

Ordinary QCD phenomenology already distinguishes what is internally present (colored quarks and gluons) from what is externally observable (color-singlet hadrons). The UNNS reading of this distinction is that internal reality and external admissibility are separate properties of a route, and that a route which cannot be admissibly externalized does not simply fail — it is repaired into a different, admissible route. The complete chain is:

$$\begin{gathered}\text{internal colored coordinate} \to \text{attempted route extension}\\ \to \text{localized route tension} \to \text{repair-threshold window}\\ \to \text{admissible color-neutral composite route.}\end{gathered}$$

This chain is the single thesis of the paper. Sections §3–§6 develop it conceptually; §7–§9 report the bounded diagnostic support for it; §10–§12 place it in context, state its limits, and close.

1.3 Two layers, kept separate

Throughout, two layers of claim are kept explicitly distinct:

Layer I — Conceptual principle. Admissibility-by-closure: internal reality does not entail external admissibility; inadmissible routes are repaired, not merely forbidden.

Layer II — Diagnostic support. Static spectra, flux-tube profiles, the repair-threshold window, the derived coordinate $\Pi_{\text{boundary}}(r)$, and the STRUC-I / STRUC-PERC-I chamber results.

Layer II does not prove Layer I. It supports a diagnostic reading of Layer I within a specific, source-indexed corpus. This distinction is maintained for the remainder of the paper.

1.4 UNNS terminology in standard physics language

The UNNS terms used in this manuscript are structural analogies, not dynamical identifications. The following dictionary is used throughout to reduce the gap between the UNNS route language and standard confinement terminology.

These correspondences organize the diagnostic reading only. They do not replace the QCD dynamical account, and none of the UNNS terms is introduced as a new physical force or potential.

Table 1: UNNS terminology mapped to standard physics language in this manuscript.

UNNS term	**Standard physics analogue used here**
route	flux configuration, channel, or ordered structural path
route extension	increasing static-source separation or attempted externalization
route tension	flux-tube localization / stored field energy
repair-threshold window	string-breaking or screening region
closure repair	quark–antiquark creation into color-neutral composites
admissible composite route	externally observable color-singlet hadron channel
boundary pressure	diagnostic stress near an inadmissible externalization boundary

2 Minimal QCD Background: Color, Confinement, and String Breaking

Quarks and gluons carry color charge, a conserved quantum number of the $SU(3)$ gauge group of the strong interaction. Unlike electric charge, color charge is never observed in isolation: every long-lived hadron is a color singlet, whether a quark–antiquark meson or a three-quark baryon. This absence of free color in the observable spectrum is what "confinement" denotes, independent of which specific dynamical mechanism is invoked to explain it.

A standard diagnostic for confinement is the static quark–antiquark potential, obtained from the energy of a pair of infinitely heavy (static) color sources separated by a distance r. At short distances the potential is Coulomb-like; at intermediate distances it rises approximately linearly, consistent with a confining flux tube connecting the sources; at sufficiently large r, the energy stored in the flux tube becomes large enough that it is energetically favored for the tube to break by creating a light (or strange) quark–antiquark pair from the vacuum, converting the stretched two-source system into two color-neutral mesons. This is *string breaking*, and the point at which it becomes energetically preferred is a *screening* or *string-breaking threshold*. The reference lattice studies used in this manuscript's diagnostic package — Bulava et al. (2019) on string breaking by light and strange quarks, Bulava et al. (2024) on the quark-mass dependence of the static potential, Baker et al. (2024) on the flux-tube structure in full QCD, and Cardoso et al. (2013) on the pure-gauge $SU(3)$ flux tube — are standard references for exactly this phenomenology [1, 2, 3, 4].

None of this manuscript's UNNS content changes, derives, or extends this physics. It is recounted here only so that §5–§6 can be read as a structural relabeling of already-established phenomenology, not as new physical content.

3 UNNS Concepts: Internal Reality, External Admissibility, Route Closure

The UNNS substrate distinguishes three properties of any ordered physical sequence or "route":

Internal reality. A coordinate, state, or constituent may be genuinely present within a system's internal structure, regardless of whether it is ever directly observable in isolation.

External admissibility. Not every internally real coordinate is an admissible output of the system when extended toward external observation. Some routes are internally real but externally inadmissible in isolation.

Route closure. When a route's natural extension is externally inadmissible, the route is not simply blocked; under UNNS admissibility-by-closure, it is repaired into a different route that *is* admissible, typically a composite formed from the original coordinate and newly generated constituents.

Two chamber instruments are used to test these properties on a given ladder of values: **STRUC-I** evaluates admissibility under perturbation, returning a regime/state classification and an admissibility coefficient $A_\kappa \in [0, 1]$ (with $A_\kappa = 1$ denoting perfect stability under the tested perturbation); and **STRUC-PERC-I** evaluates gap-connectivity of the same ladder, returning a percolation verdict (e.g. FULL_PERCOLATION or HARD_FRAGMENTATION), a giant-component ratio, and a connectivity statistic κ_{connect}. A ladder that is simultaneously STRUC-I stable and STRUC-PERC-I fully connected is, in UNNS terms, both internally coherent and structurally closed.

4 Color Confinement as Admissibility-by-Closure

Principle 1 (Admissibility-by-Closure in Color Confinement)**.** *Internal reality does not entail external admissibility. Colored constituents (quarks, gluons) are internally real, but isolated colored externalization is not an admissible output of the system. The observable route is instead tensioned, localized, and repaired into a color-neutral composite channel:*

$$\begin{gathered}\textit{internal colored coordinate} \to \textit{attempted route extension} \\ \to \textit{localized route tension} \to \textit{repair-threshold window} \\ \to \textit{admissible color-neutral composite route.}\end{gathered}$$

Table 2 sets out the correspondence between the QCD phenomenology of §2 and the UNNS reading proposed here. The mapping is a relabeling of established phenomenology in UNNS structural language; it introduces no new physical content.

Table 2: QCD confinement objects and their UNNS reading.

QCD confinement object	**UNNS reading**
Colored quark / gluon	Internally real route-coordinate
Isolated color charge	Externally inadmissible primitive
Color-neutral hadron	Admissible closed composite
Static Q–$\bar{Q}$ separation r	Route-extension coordinate
Static spectrum $V_0(r), V_1(r), V_2(r)$	Boundary-pressure / route-tension spectrum
Flux tube	Localized route tension
Flux-tube transverse profile $E_x(x_t)$	Localized route geometry
String-breaking threshold	Repair-threshold marker
Quark–antiquark pair creation	Closure repair
Two-meson / screened channel	Repaired admissible composite channel
Absence of free quarks in the spectrum	Observability constrained by admissibility, not raw non-existence

Read this way, confinement is not merely "quarks cannot escape." It is a structural statement: the escape route is inadmissible in isolation, and the system is observed to repair rather than simply suppress it.

5 Boundary Tension and Closure Repair

5.1 Repair instead of illegal decomposition

The UNNS reading of string breaking is deliberately not phrased as a forbidden decomposition. It is not:

$$\text{hadron} \;\to\; \text{free quark} + \text{free quark (forbidden)}.$$

It is:

$$\begin{aligned}\text{hadron under separation} &\to \text{route tension}\\ &\to \text{pair creation} \to \text{new hadrons}.\end{aligned}$$

Observation 1. *A boundary violation does not necessarily destroy structure; it may force recomposition into a new admissible closure. Confinement, on this reading, is not merely prohibitive — it is reparative.*

This is the conceptual center of the manuscript, and the reason "admissibility-by- closure" rather than "admissibility-by-prohibition" is the operative term: the static $Q\bar{Q}$ system does not simply fail to separate; it is repaired into two color-neutral composites once the flux-tube tension crosses a threshold.

5.2 Repair-threshold markers

Table 3 reports the two repair-threshold markers used in the diagnostic package, drawn from the light and strange static-light screening channels reported in Bulava et al. (2019) [1]. Both are treated here as repair-threshold markers, not as free-color externalization points: at each, the gap between adjacent static levels compresses and reorganizes, consistent with a channel crossing into a screened, color-neutral configuration.

Table 3: Reported repair-threshold markers (diagnostic reading).

Symbol	Channel	Reported r [fm]	$V_1 - V_0$ [GeV]	$V_2 - V_1$ [GeV]	$d(\text{gap}_{01})/dr$	$d(\text{gap}_{12})/dr$
r_c	light static-light	1.224 ± 0.015	0.0897	0.0459	-0.2114	-0.2126
r_{cs}	strange static-strange	1.293 ± 0.016	0.0864	0.0464	-0.0158	$+0.3857$

The UNNS reading of both rows is the same repair chain: stretched color route → threshold-window approach → competing screened channel → repaired admissible color-neutral composite route.

6 Visual Abstract: Admissibility-by-Closure in Color Confinement

7 Diagnostic Support: Static Spectra, Flux Profiles, and $\Pi_{\text{boundary}}(r)$

This section reports Layer II diagnostic material. None of it is offered as proof of §4–§5; it is offered as source-indexed support for a diagnostic reading of those sections, within a bounded and explicitly documented corpus.

7.1 Static spectrum

The diagnostic corpus contains 57 static energy-level rows spanning a separation range of 0.707–1.607 fm, model-reconstructed by diagonalizing the published 3×3 Hamiltonian of Bulava et al. (2019) [1]. These are not raw GEVP lattice points (see §9).

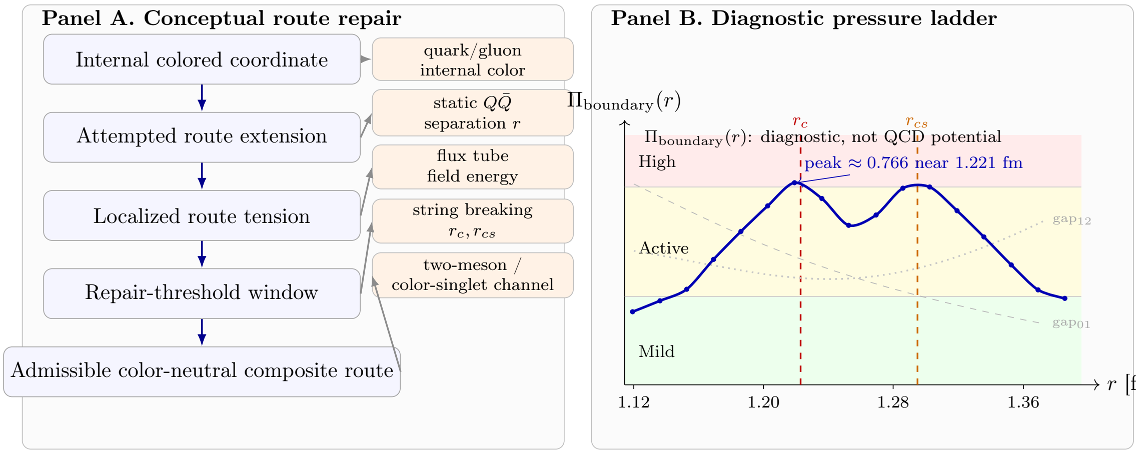

Figure 1: Expanded visual abstract: conceptual chain and diagnostic realization. (A) An internally real colored coordinate is not externally admissible in isolation; attempted extension localizes as route tension and repairs through color-neutral composite closure. (B) The derived $\Pi_{\text{boundary}}(r)$ ladder peaks near the light-channel repair threshold and forms a stable, fully connected chamber ladder. The pressure plot is schematic and diagnostic: it is not a fitted QCD law or a QCD potential.

7.2 Flux-tube profiles

1,090 pointwise flux-tube rows were parsed from 10 author-ancillary source files (Baker et al. 2024 [3]), covering 41 candidate transverse profiles. Quality control classified these as 30 Accept_for_Trend, 9 Review_Separately, and 2 Exclude_from_Trend. At the reference source separation of 0.738 fm, the peak transverse field is 0.343 GeV^2 for the full profile and 0.245 GeV^2 for its non-perturbative (NP) component, with an NP full-width-at-half-maximum estimate of 0.551 fm.

Table 4 summarizes the trusted trend dataset (Accept_for_Trend rows only, $d = 0.723$–1.060 fm), and Table 5 reports descriptive (not fitted) trend slopes on that same trusted subset.

Table 4: Trusted flux-tube trend dataset (Accept_for_Trend only).

Component	n	d range [fm]	peak range [GeV^2]	FWHM range [fm]	mean area
FULL	15	0.723–1.060	0.195–0.387	0.530–0.663	0.195
NP	15	0.723–1.060	0.126–0.274	0.544–0.723	0.152

The NP trend-statistics count and the NP chamber-ladder count differ because the chamber inputs were generated from the stricter single-column ladder-filtering pass. The chamber results therefore use the counts reported in Table 7.

The descriptive reading is that peak field weakens and width broadens modestly with increasing separation. This is interpreted as route redistribution, not route disappearance, consistent with §5's repair framing rather than a simple decay picture. The remaining 9 Review_Separately rows (3 qualitative string-breaking profiles, 2 boundary/noise-dominated rows, 2 low-SNR rows pending normalization, 1 large-distance control, 1 outlier note) are held as a separate evidence class and are not discarded, but are excluded from the trend statistics above and from the chamber ladders below.

Table 5: Descriptive trend slopes, trusted rows only. Not a fitted physical law.

Component	Quantity	Slope vs. d	Correlation r
FULL	peak	−0.4885	−0.960
FULL	fwhm	+0.3711	+0.964
FULL	area	−0.1919	−0.969
NP	peak	−0.2939	−0.908
NP	fwhm	+0.4207	+0.928
NP	area	−0.0818	−0.825

7.3 The derived coordinate $\Pi_{\text{boundary}}(r)$

A single derived diagnostic coordinate is constructed from the QC-accepted static ladder (17 rows in the repair-window region):

$$\Pi_{\text{boundary}}(r) = w_{\text{gap}} C_{\text{gap}}(r) + w_{\text{thr}} C_{\text{threshold}}(r) + w_{\text{slope}} C_{\text{slope}}(r),$$
$$w_{\text{gap}} = 0.412, \qquad w_{\text{thr}} = 0.353, \qquad w_{\text{slope}} = 0.235.$$

where C_{gap} is channel-gap compression near r_c/r_{cs}, $C_{\text{threshold}}$ is proximity to the nearest repair marker, and C_{slope} is finite-difference gap-reorganization sharpness. A flux term C_{flux} was deliberately withheld from this first executable pass and remains symbolic (weight 0.15 in the underlying v0.1 definition). This working definition (version `v0.3.0`, `STATIC_ONLY_EXACT_COLUMNS`) is explicitly framed as a derived diagnostic coordinate designed to test whether repair-window information can be coordinatized into a stable UNNS boundary-pressure ladder — it is not a fitted physical law and not a QCD potential.

Over the 17-row repair-window ladder, mean $\Pi_{\text{boundary}}(r) = 0.546$, with a minimum of 0.278 at $r = 1.125$ fm and a maximum of 0.766 at $r = 1.221$ fm. A methodological (not physically calibrated) three-band classification places 7 rows in Mild_Tension, 9 in Active_Repair_Window, and 1 in High_Near_Repair — the single high-band row, at $r = 1.22094$ fm, sits immediately adjacent to the reported light-channel threshold $r_c = 1.224$ fm (Table 3). Table 6 shows selected rows spanning both reported thresholds.

Table 6: $\Pi_{\text{boundary}}(r)$ near the repair window (selected rows).

r [fm]	gap_{01} [GeV]	gap_{12} [GeV]	Π_{boundary}	Band
1.12455	0.1449	0.0619	0.278	Mild
1.17275	0.1096	0.0558	0.477	Mild
1.18881	0.1009	0.0529	0.583	Active
1.20488	0.0942	0.0495	0.679	Active
1.22094	0.0897	0.0459	**0.766**	High (near r_c)
1.28520	0.0864	0.0464	0.745	Active (near r_{cs})
1.30127	0.0860	0.0543	0.750	Active
1.38159	0.0827	0.1202	0.328	Mild

8 Chamber Result: Stability and Connectivity of the Derived Boundary Coordinate

Nine chamber-ready single-column ladders, all derived from QC-accepted rows only, were evaluated under both instruments. Table 7 reports all nine.

Table 7: STRUC-I × STRUC-PERC-I results, all 9 ladders.

Ladder	n	STRUC-I regime/state	mean A_κ	min A_κ	STRUC-PERC-I verdict	giantRatio	κ_{connect}
flux_FULL_area_trusted	15	GP / Weak Persist.	0.99996	0.9990	FULL_PERCOLATION	1.000	40.02
flux_FULL_peak_trusted	15	GP / Weak Persist.	0.95826	0.8605	HARD_FRAGMENTATION	0.857	—
flux_FULL_width_trusted	15	GP / Weak Persist.	0.99999	0.9995	HARD_FRAGMENTATION	0.857	—
flux_NP_area_trusted	13	GP / Weak Persist.	0.99974	0.9975	FULL_PERCOLATION	1.000	10.00
flux_NP_peak_trusted	13	GP / Weak Persist.	0.99558	0.9805	FULL_PERCOLATION	1.000	4.01
flux_NP_width_trusted	13	GP / Weak Persist.	1.00000	1.0000	HARD_FRAGMENTATION	0.923	—
static_gap01_repair_window	17	GP / Stable Structure	0.99849	0.9740	FULL_PERCOLATION	1.000	10.00
static_gap12_repair_window	17	GP / Stable Structure	1.00000	1.0000	HARD_FRAGMENTATION	0.941	—
$\Pi_{\text{boundary}}(r)$	17	GP / Stable Structure	**1.00000**	1.0000	FULL_PERCOLATION	**1.000**	10.00

GP = Geometric Persistence. Flux ladder n reflects the ACCEPT_FOR_TREND counts recorded at chamber-input generation time (13 for the NP component; cf. Table 4, which reports 15 NP profiles at the trend-statistics stage).

Table 8: Descriptor classes and chamber interpretation.

Descriptor class	**STRUC-I behavior**	**STRUC-PERC-I behavior**	**UNNS interpretation**
Local shape descriptors (peak/width)	admissible	often fragmented	localized route geometry; sensitive to profile shape and sampling
Global descriptors (area/gap$_{01}$)	admissible	often connected	integrated route coherence; less sensitive to local profile shape
Derived coordinate $\Pi_{\text{boundary}}(r)$	perfect stability	full percolation	coordinatized boundary pressure; closed diagnostic route

The derived coordinate therefore performs a structural integration analogous to the confinement reading itself: local components need not individually externalize as stable global descriptors, but their repair-window organization can close into a single admissible diagnostic coordinate. In this limited sense, $\Pi_{\text{boundary}}(r)$ is not another local observable; it is a coordinatized closure of the repair-window information. The withheld flux term in the first executable definition is a modular design choice: future versions can add normalized flux information without changing the static-only evidentiary boundary of the present manuscript.

Finding 1. *Four of eight raw local-descriptor ladders reach* HARD_FRAGMENTATION *under STRUC-PERC-I (flux_FULL_peak, flux_FULL_width, flux_NP_width, static_gap12) despite being individually STRUC-I admissible; the other four (flux_FULL_area, flux_NP_area, flux_NP_peak, static_gap01) reach* FULL_PERCOLATION*. The pattern separates global route-integral coherence (area, gap$_{01}$) from local shape sensitivity (peak, width, gap$_{12}$), and motivates constructing a single coordinatizing observable rather than reading any one raw ladder as "the" confinement signal.*

Finding 2. $\Pi_{\text{boundary}}(r)$ *is the strongest chamber result in the color-confinement chain. It is simultaneously STRUC-I* Geometric Persistence / Stable Structure *(mean $A_\kappa = 1.000$, min $A_\kappa = 1.000$) and STRUC-PERC-I* FULL_PERCOLATION (giantRatio = 1.000, $\kappa_{\text{connect}} = 10$*, 0 isolated nodes of 17). No raw local descriptor in the package achieves the same exact joint profile: perfect STRUC-I stability with min $A_\kappa = 1.000$ and STRUC-PERC-I* FULL_PERCOLATION*. The derived coordinate therefore acts as a coordinatizing observable: it takes partially fragmented lower-level descriptors (flux peak/width, static gap$_{12}$) and produces* *a stable, fully connected pressure coordinate, with its peak value (*0.766*) falling at* $r = 1.221$ *fm — adjacent to the reported light-channel repair threshold* $r_c = 1.224$ *fm.*

This is a legitimate internal chamber result: the derived coordinate $\Pi_{\text{boundary}}(r)$ is well-behaved under both instruments. It is not, on its own, evidence for or against any QCD dynamical mechanism; it is evidence that the UNNS repair-window construction is coordinatizable in a stable, connected way over this corpus.

9 Data Status and Evidentiary Boundary

This subsection is deliberately explicit, since the diagnostic material in §7–§8 is only as trustworthy as its documented provenance.

- The static-source energy levels used here (§7.1, Table 3) are `Model_Reconstruction_from_Reported_Parameters_Not_Raw_Data`: they are diagonalized from the published 3×3 Hamiltonian of Bulava et al. (2019) [1], not raw GEVP lattice points.
- The Baker flux-tube profiles (§7.2) are `Author_Ancillary_Pointwise_Data` [3]: author-supplied pointwise files, suitable for diagnostic support only after the quality-control pass reported in §7.2 (30 accept / 9 review-separately / 2 exclude, of 41 profiles).
- Every row in the underlying package carries a source identifier, a source URL/arXiv/DOI, a source location, and a `row_provenance` tag drawn from a controlled vocabulary of nine values, documented in an accompanying data-status guide.
- Cardoso et al. (2013) [4] is registered as a secondary, pure-gauge control source but has not yet been extracted into any data table used here.
- The package as a whole is documented, in its own provenance records, as a *seed pack* — a source-indexed, QC-annotated diagnostic starting point — and explicitly not as a raw lattice-data repository [5].

Therefore, the empirical material in §7–§8 is not presented as a new lattice-QCD analysis. It is presented as a source-indexed UNNS diagnostic exercise, bounded by the provenance status of every row it uses. The following non-claims hold throughout this manuscript and are restated in §11:

- This manuscript does not derive QCD confinement.
- $\Pi_{\text{boundary}}(r)$ is not a physical QCD potential.
- The weights in the $\Pi_{\text{boundary}}(r)$ definition are not universal; they are specific to this working definition (`v0.3.0`).
- The static-only proxy is not a final theory of confinement.

9.1 Limits and future diagnostic extensions

The static-only proxy is deliberately incomplete. The term C_{flux} was withheld from the first executable pass so that the initial test could be run on an exact-column static repair-window table without mixing provenance classes. This makes the current result cleaner, but it also defines the next diagnostic target: a multi-component version of $\Pi_{\text{boundary}}(r)$ with a normalized flux contribution should be tested for robustness under small provenance and QC variations.

Three queued extensions follow directly from the seed package: (i) extraction of the Cardoso et al. pure-gauge control source, which is registered but not yet used in any table; (ii) deeper use of the Bulava et al. 2024 physical-point and quark-mass-dependence material; and (iii) broader pointwise flux coverage across source separations and profile classes. These are future diagnostic extensions, not prerequisites for the present conceptual claim.

10 Relation to Boundary-Route Preservation

The present color-confinement reading is parallel to, but distinct from, the Charge Boundary-Route Preservation Law. In the charge-routing case, scalar charge conservation is the visible projection, while boundary-route preservation is the structural invariant. Equal scalar charge does not imply equal structural route, and charge-balanced candidate transitions can remain graph-connected while losing perturbative route admissibility [7, 6].

Color confinement supplies a complementary physical analogue. A colored quark coordinate is internally real, just as a fractional charge coordinate is internally valid, but neither is an admissible free external closure. The admissible output is not the isolated primitive; it is the closed composite route. Thus both manuscripts support the same UNNS distinction: local value or constituent identity is insufficient unless the route closes.

The relation can be stated compactly:

charge routing:	scalar charge value	is not the full route,
color confinement:	colored constituent identity	is not the external closure.

In both cases, the visible projection is necessary but structurally incomplete. The manuscript therefore uses the charge-boundary law only as a programmatic parallel. It does not import the charge corpus into the color-confinement result, and it does not claim that electric charge routing and color confinement are the same physical mechanism.

11 Limitations: Boundary of the Claim

- This manuscript does not solve confinement.
- It does not derive the QCD mass gap.
- It does not replace the gauge-theoretic account of color confinement.
- It does not use raw GEVP tables; the static spectrum is model-reconstructed from published parameters (§9).
- It does not claim that $\Pi_{\text{boundary}}(r)$ is a physical potential or a physical law.
- Only one Baker flux-tube profile family has full pointwise coverage in the underlying corpus; the pure-gauge control source (Cardoso 2013) remains unextracted.

The positive claim, stated plainly, is narrower than any of the above might suggest it needs to be: this manuscript identifies color confinement as a benchmark case where internal reality, external admissibility, and closure repair are physically separated, and shows that a single derived UNNS coordinate built from that separation is chamber-stable and fully connected over the tested corpus.

12 Conclusion

Color confinement, read through the UNNS substrate, is admissibility-by-closure:

$$\begin{gathered}\text{internal colored coordinate} \to \text{attempted route extension} \\ \to \text{localized route tension} \to \text{repair-threshold window} \\ \to \text{admissible color-neutral composite route.}\end{gathered}$$

The isolated colored route is not externalized; it localizes as flux-tube tension; the repair window reorganizes channel structure; the admissible continuation is color-neutral closure. The derived coordinate $\Pi_{\mathrm{boundary}}(r)$, built only from static-source diagnostic data, is chamber-stable under STRUC-I ($A_\kappa = 1.000$) and fully connected under STRUC-PERC-I (giantRatio $=$ 1.000) — the first explicit UNNS confinement-pressure coordinate in the program, and, on the tested corpus, its strongest chamber result.

This manuscript does not derive QCD confinement, does not claim $\Pi_{\mathrm{boundary}}(r)$ as a physical potential, and does not treat its diagnostic package as a substitute for raw lattice-QCD data. Its contribution is the structural relabeling of §4 and the bounded diagnostic demonstration of §7–§8, kept explicitly separate throughout.

The color-confinement result motivates later cross-regime tests, including H-mode plasma confinement, where an edge-admissibility margin $m_{\mathrm{edge,event}}$ may be compared against $\Pi_{\mathrm{boundary}}(r)$. That comparison is a planned extension, not a result of this manuscript, and is deliberately left outside its scope.

Data Availability

The `color_confinement_data_seed_v0.1.1_provenance` package, including source registry files, QC tables, chamber-ready ladders, chamber outputs, diagnostic reports, and reconstruction scripts, is available as supplementary material. The package is a source-indexed diagnostic seed and not a raw lattice-data repository.

A Provenance Summary

Table 9 summarizes the principal data objects used by the manuscript. The table is intentionally compact; detailed row-level provenance is kept in the companion seed package.

Table 9: Principal provenance objects and manuscript use.

Object	Source type	Rows / count	Provenance status	Manuscript use
`source_registry.csv`	source registry	4 primary references	controlled source index	source identity, arXiv/DOI/URL, extraction status
`bulava2019_model_reconstructed_pointwise_E_levels.csv`	static spectrum table	57 rows	model reconstruction, not raw GEVP	static spectrum and threshold-window context
`repair_threshold_window_static_gaps.csv`	static repair-window table	17 rows	model reconstruction, not raw GEVP	construction of $\Pi_{\mathrm{boundary}}(r)$
`baker2024_extended_flux_profiles_long.csv`	author-ancillary pointwise profiles	1,090 rows / 41 profiles	author ancillary; QC required	flux-tube separation extension and profile trends
`baker_flux_profile_trusted_summary.csv`	QC-filtered flux summary	30 accepted trend rows	QC accepted for trend	flux area/peak/width chamber ladders
STRUC-I / STRUC-PERC-I chamber outputs	derived chamber diagnostics	9 ladders	derived from QC-accepted inputs	admissibility and connectivity verdicts

B Selected $\Pi_{\mathrm{boundary}}(r)$ ladder values

Table 10 gives the 17-row static-only boundary-pressure ladder used for the derived-coordinate chamber test. Values are dimensionless except for r and the two energy gaps.

References

[1] J. Bulava, B. Hörz, F. Knechtli, V. Koch, G. Moir, C. Morningstar, and M. Peardon. String breaking by light and strange quarks in QCD. *Phys. Lett. B*, *arXiv:1902.04006*,

Table 10: Static-only $\Pi_{\text{boundary}}(r)$ ladder values.

r [fm]	gap_{01}	gap_{12}	C_{gap}	C_{thr}	C_{slope}	Π_{boundary}	Band
1.12455	0.1449	0.0619	0.368	0.000	0.536	0.278	Mild
1.14061	0.1320	0.0602	0.482	0.000	0.511	0.319	Mild
1.15668	0.1201	0.0582	0.590	0.024	0.478	0.364	Mild
1.17274	0.1096	0.0558	0.689	0.257	0.435	0.477	Mild
1.18881	0.1009	0.0529	0.778	0.490	0.380	0.583	Active
1.20487	0.0942	0.0495	0.853	0.723	0.310	0.679	Active
1.22094	0.0897	0.0459	0.912	0.956	0.225	0.766	High
1.23700	0.0874	0.0427	0.951	0.812	0.125	0.707	Active
1.25307	0.0866	0.0409	0.968	0.579	0.012	0.606	Active
1.26913	0.0865	0.0419	0.963	0.654	0.078	0.646	Active
1.28520	0.0864	0.0464	0.935	0.887	0.200	0.745	Active
1.30126	0.0860	0.0543	0.889	0.880	0.310	0.750	Active
1.31733	0.0854	0.0648	0.828	0.647	0.391	0.661	Active
1.33340	0.0847	0.0771	0.756	0.415	0.444	0.562	Active
1.34946	0.0839	0.0906	0.676	0.182	0.479	0.455	Mild
1.36553	0.0833	0.1051	0.590	0.000	0.503	0.361	Mild
1.38159	0.0827	0.1202	0.500	0.000	0.519	0.328	Mild

2019.

[2] J. Bulava, F. Knechtli, V. Koch, C. Morningstar, and M. Peardon. The quark-mass dependence of the potential energy between static colour sources in the QCD vacuum with light and strange quarks. *Phys. Lett. B*, *arXiv:2403.00754*, 2024.

[3] M. Baker, P. Cea, V. Chelnokov, L. Cosmai, and A. Papa. Unveiling the flux tube structure in full QCD. *Eur. Phys. J. C*, *arXiv:2409.20168*, 2024.

[4] N. Cardoso, M. Cardoso, and P. Bicudo. Inside the SU(3) quark-antiquark QCD flux tube: screening versus quantum widening. *Phys. Rev. D*, *arXiv:1302.3633*, 2013.

[5] UNNS Substrate Research Program. Color Confinement — UNNS Analytics: Content Analytics for the Color Confinement Data Seed (v0.1.1). *UNNS Corpus Analytics Dashboard*, 12 July 2026.

[6] UNNS Substrate Research Program. Charge Boundary Routing: Fractional Coordinates, Composite Closure, and Route-Preserving Transitions. *UNNS Working Manuscript*, 2026.

[7] UNNS Substrate Research Program. The Charge Boundary-Route Preservation Law: Value Conservation, Route Admissibility, and Structural Selection in Charge-Bearing Transitions. *UNNS Completed Law Paper*, 2026.